

# Painometry: Wearable and Objective Quantification System for Acute Postoperative Pain

Hoang Truong<sup>1</sup>, Nam Bui<sup>1</sup>, Zohreh Raghebi<sup>4</sup>, Marta Ceko<sup>5</sup>, Nhat Pham<sup>1,2</sup>, Phuc Nguyen<sup>1,3</sup>, Anh Nguyen<sup>1</sup>, Taeho Kim<sup>1</sup>, Katrina Siegfried<sup>4</sup>, Evan Stene<sup>4</sup>, Taylor Tvrdy<sup>5</sup>, Logan Weinman<sup>5</sup>, Thomas Payne<sup>1</sup>, Devin Burke<sup>1</sup>, Thang Dinh<sup>6</sup>, Sidney D’Mello<sup>5</sup>, Farnoush Banaei-Kashani<sup>4</sup>, Tor Wager<sup>7</sup>, Pavel Goldstein<sup>8</sup>, Tam Vu<sup>1,2</sup>

<sup>1</sup>University of Colorado Boulder, <sup>2</sup>University of Oxford, <sup>3</sup>University of Texas at Arlington,

<sup>4</sup>University of Colorado Denver, <sup>5</sup>Institute of Cognitive Science, University of Colorado Boulder,

<sup>6</sup>Virginia Commonwealth University, <sup>7</sup>Dartmouth College, <sup>8</sup>University of Haifa

{firstname.lastname}@colorado.edu, {firstname.lastname}@cs.ox.ac.uk, {firstname.lastname}@ucdenver.edu  
tndinh@vcu.edu, tor.d.wager@dartmouth.edu, pavelg@stat.haifa.ac.il

## ABSTRACT

Over 50 million people undergo surgeries each year in the United States, with over 70% of them filling opioid prescriptions within one week of the surgery. Due to the highly addictive nature of these opiates, a post-surgical window is a crucial time for pain management to ensure accurate prescription of opioids. Drug prescription nowadays relies primarily on self-reported pain levels to determine the frequency and dosage of pain drug. Patient pain self-reports are, however, influenced by subjective pain tolerance, memories of past painful episodes, current context, and the patient’s integrity in reporting their pain level. Therefore, objective measures of pain are needed to better inform pain management.

This paper explores a wearable system, named Painometry, which objectively quantifies users’ pain perception based on multiple physiological signals and facial expressions of pain. We propose a sensing technique, called sweep impedance profiling (SIP), to capture the movement of the facial muscle corrugator supercilii, one of the important physiological expressions of pain. We deploy SIP together with other biosignals, including electroencephalography (EEG), photoplethysmogram (PPG), and galvanic skin response (GSR) for pain quantification.

From the anatomical and physiological correlations of pain with these signals, we designed Painometry, a multimodality sensing system, which can accurately quantify different levels of pain safely. We prototyped Painometry by building a custom hardware, firmware, and associated software. Our evaluations use the prototype on 23 subjects, which corresponds to 8832 data points from 276 minutes of an IRB-approved experimental pain-inducing protocol. Using leave-one-out cross-validation to estimate performance on unseen data shows 89.5% and 76.7% accuracy of quantification under 3 and 4 pain states, respectively.

Permission to make digital or hard copies of all or part of this work for personal or classroom use is granted without fee provided that copies are not made or distributed for profit or commercial advantage and that copies bear this notice and the full citation on the first page. Copyrights for components of this work owned by others than ACM must be honored. Abstracting with credit is permitted. To copy otherwise, or republish, to post on servers or to redistribute to lists, requires prior specific permission and/or a fee. Request permissions from [permissions@acm.org](mailto:permissions@acm.org).

*MobiSys '20, June 15–19, 2020, Toronto, ON, Canada*

© 2020 Association for Computing Machinery.

ACM ISBN 978-1-4503-7954-0/20/06...\$15.00

<https://doi.org/10.1145/3386901.3389022>

## CCS CONCEPTS

• **Computer systems organization** → **Embedded systems**; • **Human-centered computing** → **Mobile devices**; • **Hardware** → **Sensor devices and platforms**.

## KEYWORDS

impedance sensing, pain quantification, opioid overdose

## ACM Reference Format:

Hoang Truong, Nam Bui, Zohreh Raghebi, Marta Ceko, Nhat Pham, Phuc Nguyen, Anh Nguyen, Taeho Kim, Katrina Siegfried, Evan Stene, Taylor Tvrdy, Logan Weinman, Thomas Payne, Devin Burke, Thang Dinh, Sidney D’Mello, Farnoush Banaei-Kashani, Tor Wager, Pavel Goldstein, Tam Vu. 2020. Painometry: Wearable and Objective Quantification System for Acute Postoperative Pain. In *The 18th ACM International Conference on Mobile Systems, Applications, and Services (MobiSys’20), June 15-19, 2020, Toronto, Canada*. ACM, New York, NY, USA, 15 pages. <https://doi.org/10.1145/3386901.3389022>

## 1 INTRODUCTION

In recent decades, the United States has faced an opioid epidemic, with 40,000 lives lost annually due to opioid misuse [25, 99]. It is estimated that around 25% of patients who have been prescribed opioids for pain misuse them [111], about 5% of the misusers escalate to heroin, and about 10% of them develop an opioid addiction. In addition, about 80% of people who use heroin have previously misused prescription opioids [13, 17, 45]. Over 50 million people undergo surgeries each year [37] in the United States, with over 70% of them filling opioid prescriptions after surgery [54].

Due to the highly addictive nature of these opiates, the post-surgical window is a crucial time for pain management to ensure accurate prescription of opioids. However, a critical challenge in pain management emerges from the fact that pain cannot be directly measured without invasively accessing the nervous system [89]. Therefore, the current non-invasive gold standard for the assessment of pain is the patient self-report of pain intensity [10]. Though pain self-reporting is a common measure that reflects a patient’s conscious perception of the given painful sensation, it has several significant limitations, especially for long-term usage: (1) self-reporting is subjective and is influenced by the patient’s cognitive

load and emotion at the time of reporting [64, 78, 79], (2) self-reporting introduces bias since frequent self-reporting of pain can create pain perception [39], and (3) self-reporting cannot be assessed frequently or continuously as this would present an unrealistic burden on the patient.

Thus, there is a critical need for a more objective measure of pain that is efficacious and convenient for real-world daily usage. Common biosignals that have shown potential in capturing pain-related neurophysiological processes include electroencephalography (EEG), electromyography (EMG), Galvanic Skin Response (GSR), electrocardiography (ECG), and photoplethysmogram (PPG). The most accurate and objective pain quantification approach is using a fMRI machine [84]. However, this approach is expensive and inconvenient since it is only available in a clinical setting. Studies have used multiple features extracted from facial EMG (corrugator and zygomaticus muscles), GSR, and ECG signals to classify experimentally-induced pain from non-pain with accuracies ranging from 79-91% [12, 16, 33, 47, 95, 106, 110]. Further improvement of these approaches also integrates physiology-, video-, and voice-based signals to predict pain. Recent studies have fused ECG, facial EMG, GSR, and video data to achieve 80-84% accuracy in discriminating experimental pain vs. non-pain [46, 48, 62]. However, these systems are often cumbersome because they require complicated to setup, and do not support mobility settings.

In this work, we propose Painometry (Fig. 1), a multimodal sensing system for objective pain quantification that can be integrated into various form factors (e.g. hat, headband, etc.). The key idea is to capture the core signals that are directly correlated to pain perception, namely the facial muscle activity above and between our eyes, in combination with a small number of less pain-specific signals. The light-weight form factor and a minimal number of sensors enable the mobility of Painometry and its capability as a wearable and daily device. Painometry aims to support a wide range of applications, including in-hospital scenarios such as automatically and objectively answering the pain rating assessment; assisting anesthetic monitoring; in-home pain assessment for accurate dosing of pain relief medication; pain management such as daily and real-time medication reminder; and, in long-term assessments, development of intervention therapies bypassing medication schedules to address chronic pain.

The key challenges in developing such a system include: (1) accurately capturing the specific muscle actively affected by the autonomous nervous system during pain; (2) identifying a set of pain-related features from multiple bio signals that are useful in providing an objective pain quantification; (3) and isolating different types of noise present in the recorded signals.

We introduce Sweep Impedance Profiling (SIP), a sensing technique that captures the minuscule movement of muscle under the point where the sensor makes contact with the skin to capture autonomous muscle activity in high spatial resolution with a small number of sensors. SIP has advantages over existing impedance-based sensing techniques in the capability of (1) measuring impedance of the singular muscle group under the skin, (2) providing more detailed information about the muscle over a range of sweeping excitation frequencies, and (3) specifying with greater precision the area of the muscle of interest. To improve the sensitivity of the system, we leverage a small number of head-based biosignals

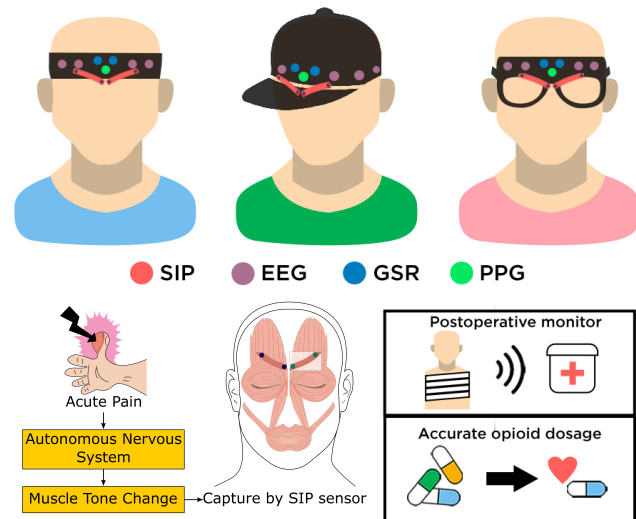


**Figure 1: Top panel: Painometry signal recording sites including positioning of PPG, GSR, EEG, and SIP sensors. Left panel: Flowchart of stimulus processing from the onset of acute pain through the autonomous nervous system (ANS) to the sensing sites of the Painometry system. Right panel: Key applications of the Painometry system include its use as a postoperative monitor, as well as in mitigation of opioid prescriptions.**

including EEG, GSR, and PPG. To objectively quantify different pain levels, we design a thorough experimental protocol to mimic acute post-surgical pain, analyze the recorded biosignal data, and build a quantification model that utilizes pain-related feature extraction and selection. We design the Painometry hardware following established safety guidelines to ensure the system will not cause any safety concerns.

Through this work, we make the following key contributions:

- Introducing a sensitive muscle activity detection technique, Sweep Impedance Profiling (SIP).
- Proposing an objective pain quantification algorithm including a wide-range pain-related feature extraction from recorded biosignals, a feature selection using a Recursive Feature Elimination (RFE) method, and a light-weight classification model.
- Evaluating pain quantification of 23 subjects in an experimental protocol to mimic post-surgical pain with the accuracy of 76.7% and 89.5% for 4 and 3 pain levels respectively under leave-one-out cross-validation.

Though at current phase, this work is limited to in-lab experiments and only targets acute pain in postoperative pain, it is the first step in a concerted effort to target different types of pain (i.e. acute and chronic) and to reduce opioid overdose by developing drug-free, fully closed-loop, and just-in-time pain coaching and intervention systems.

## 2 ANATOMY AND PHYSIOLOGY OF PAIN

In this section, we discuss the anatomy and physiology of pain to understand the activation of autonomous nervous system (ANS, Fig. 2) during pain. When activated, the ANS elicits identifiable changes in muscle tone, heart rate, skin conductance, and brain activity.

**Pain perception.** Pain is a conscious subjective experience that results from the transduction of nociceptive stimuli into neural signals that are transmitted to higher cortical brain regions [24]. The sensation of pain is the result of tightly coupled neurophysiological processes - the peripheral detection of nociceptive stimuli and the transmission and processing of these signals in the central nervous system.

**Acute postoperative pain.** Acute pain refers to the short-term effects of pain, typically lasting less than 3 months, and is directly related to soft tissue damage with sharp and dull sensations [94]. After the 3 month window, chronic pain may develop and pain can become progressively worse and reoccur intermittently. Strong correlations exist between the severity of acute postoperative pain and the development of chronic pain [80]. The postoperative time window is also a period of concern relating to opioid misuse. Most patients are subjected to opioid prescriptions following surgery, putting them at risk of dependence. According to Brat et al. [9], each additional prescription refill after surgery attributes to a 44% increase in the likelihood of opioid misuse. For these reasons, providing a quantitative method for managing the intensity of postoperative acute pain to reduce the duration of opioid prescription is the main goal of Painometry and guides the system and protocol design processes.

**Importance of objective pain quantification.** To determine patient's current pain state, physicians rely primarily on the patient's subjective self-report, typically using a pain scale (e.g., Visual analog scale (VAS) [38]). Patients' report of their pain level using the VAS is influenced not only by the current subjective level of pain but also by patients' pain tolerance, emotional state, current environment, memories of past painful episodes, and willingness to communicate painful experiences.

In addition, patients have difficulty providing a good estimate of their current pain state because they have no objective way to distinguish the score. The lack of an objective pain measurement method can lead to biased pain evaluation and as result to overdosing of patients and drug misuse [77], or underdosing and unnecessary pain for the patients. Thus, an objective pain quantification system brings benefits in (1) removing the need for a patient to verbalize and focus on their pain state, (2) improving dosing, which can reduce the risk of developing an opioid addiction while reducing patients' suffering, and (3) improving clinical and healthcare systems with reliable assessments of patient conditions.

**Noninvasive sensing of physiological pain expression.** Assessing facial expressions of pain behavior is a viable noninvasive technique to quantify pain [22]. A number of researchers have placed emphasis on universality in expressions of pain, meaning the same pattern of muscle activation consistently appears when people are experiencing pain [18, 81]. The Facial Action Coding System (FACS) [22] is a precise measurement technique that many pain studies have employed to accrue evidence that certain facial actions

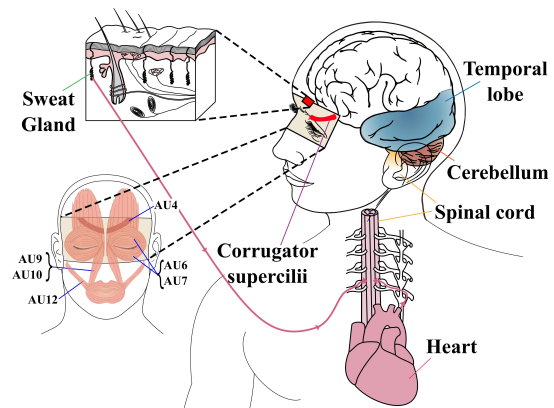


**Figure 2: Targets for autonomous nervous system pain response: corrugator supercilii, heart, sweat glands, and brain.**

are reliably correlated with pain [88]. The FACS assigns the activity of distinct facial muscle groups to 44 unique action units (AUs). Muscle groups of interest in the context of pain studies [18, 57, 81] include (Fig. 2): (i) AU4 - Brow lowering, (ii) AU6/AU7 - Orbit tightening, (iii) AU9/AU10 - Levator contraction, and (iv) AU12 - Oblique lip pulling. In developing the SIP sensor employed in Painometry, we referenced many of the protocols used by FACS to recognize and classify statistically distinct movements of the corrugator supercilii [85, 86].

The hypothalamus and limbic brain regions involved in the perception of pain are also involved in the modulation of the ANS. These regions are responsible for bodily functions that are regulated without conscious input, such as breathing, heart rate, vasomotor activities, and reflex reactions. The hypothalamus integrates regulatory input from the limbic system and regulates functions of the ANS. These autonomic responses happen with real pain only (not acted pain) and can be captured with the EEG sensor, pulse sensor, GSR sensor, and muscle activity sensor accordingly.

With the goal of having a wearable system suitable for daily usage, one of the areas where it is feasible to accommodate all those sensors is the Fpz-Oz horizontal line in the 10-20 system [40] that covers the forehead area (as depicted in Fig. 1).

We also base our choice for sensor placement on the intuition that the forehead (1) provides a good measurement for GSR [107], (2) is a common area to measure PPG signals [115], and (3) covers a part of the corrugator supercilii. Since the signals resulting from muscular contractions initiated by the autonomic innervation of corrugator supercilii are typically small compared to larger signals from neighboring facial muscles (e.g., eye blinking, eye movement, and jaw movement), the passive EMG measurement with electrodes over the eyebrow is prone to noise. Thus, there is a need for both a high spatial resolution and a sensitive measurement to capture autonomic corrugator supercilii responses. In the next section, we will discuss the overview of Painometry and our design goals.

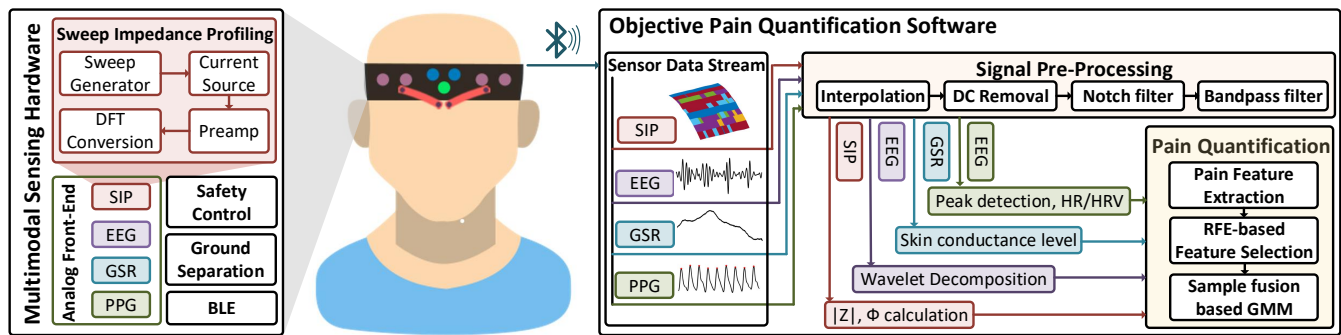


Figure 3: Painometry System Overview. Sensing data collected with multimodal sensing hardware (Left) and streamed via Bluetooth to software on host device (Right) that process data stream, extract pain features, and quantify pain level.

### 3 SYSTEM OVERVIEW

In this section, we describe the overall design of Painometry, the multimodal sensing headband for objective pain quantification based on the analysis of physiological expression of pain and autonomic responses. The design goals include (1) sensitive and high spatial resolution muscle activity sensing; (2) a reliable and safe multimodal physiological sensing system; and (3) highly accurate and light-weight pain level quantification.

**Sensitive and high spatial resolution muscle activity sensing.** Muscle activity is traditionally measured using the electromyography (EMG) technique. EMG sensors passively capture the biopotentials of the muscles under the sensing electrodes. However, the recorded signals are usually the combination of biopotentials from multiple sources due to nearby muscle activity being detected by the electrodes, which is known as cross-talk noise. One example of cross-talk noise is that the EMG sensors on the forehead also capture eye movements and blinking. In order to capture the activity of the muscle group of interest only, one of the conventional solutions is to have multiple sensors that capture biopotentials from other muscle sources and then use regression or ICA techniques to extract the necessary information [103]. However, this approach requires the addition of multiple electrodes attached to the head in order to accurately extract the EMG contribution of the corrugator supercilii group. So, in order to capture the muscle activity of the corrugator supercilii muscle with fewer sensors and to overcome the multi-source noise limitations, we explore the Sweep Impedance Profiling (SIP) sensing technique. By attaching only two sensors on top of the muscle group of interest, this sensing method can capture the change in impedance caused by the contraction of that muscle group.

**Reliable, wearable, and safe multimodal physiological sensing system.** In order to capture various physiological expressions of the human body, a conventional multimodal sensing system includes different combinations of sensing modalities such as EEG, EMG, ECG, eye tracking, facial expressions, GSR, etc. These systems are popular in many mental health and cognitive-related research and application such as stress detection [6, 51], seizure prediction [34, 108], and sleep monitoring [19, 20, 72]. Existing pain-sensing applications analyze individual bio-signals or different combinations of EEG, EMG, GSR, and PPG to explore distinctive

features among different pain states [50, 71, 75]. However, there are challenges in bringing all mentioned sensors together in a singular wearable hardware device that satisfies a daily usage scenario. In particular, integrating multiple sensors on a small-size hardware is prone to cross-talk interference noise. In addition, the GSR and SIP sensors that we employ are considered ‘active’ sensors where a current runs through part of a human body. Thus, it is required to consider safety constraints. We carefully design our multimodal sensing system including SIP, EEG, GSR, and PPG to minimize the cross-talk noise and restrict the ‘active’ sensors under safety thresholds.

**Highly accurate pain level quantification.** The main challenge in building the pain quantification system is the subjective nature of pain perception. Another challenge is determining distinctive features among different pain states. Existing work provides various findings in pain-related feature extraction from multiple sensors, however, there is no universally common feature set that we can directly employ into our work. We thoroughly design an experimental pain-inducing device and data collection protocol to obtain highly accurate ground truth labels. We extract a set of possible features from each corresponding biosignal and use a recursive feature elimination as a feature selection algorithm to identify the most discriminating set of features. Finally, we aggregate all the features within one chunk of data to create the sample for our learning model.

**Painometry System.** Fig. 3 illustrates two main components of Painometry including (1) a wearable multi-modal sensing device to capture physiological pain expression, and (2) an Objective Pain Quantification Software running on the host computer (i.e., mobile phones or PCs). Painometry hardware can be integrated into various form factors (e.g. hat, headband, or eye-glass). The host device receives the streaming data from all the sensors, processes the data, and quantifies the current pain level of the user. There are three sub-components of the Painometry’s software architecture including (1) Signal pre-processing, (2) Dedicated sensor feature analysis, and (3) Pain quantification algorithm. In the following discussion, we will describe these sensing hardware and software components in details.

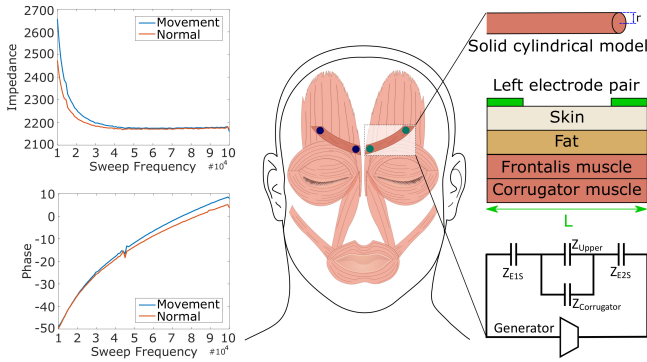


**Figure 4: SIP sensors over corrugator supercillii and the corresponding circuit.**

#### 4 SWEEP IMPEDANCE PROFILING

As stated in previous sections, we seek an accurate and sensitive muscle activity detection method which requires minimal electrodes and fits into a wearable form factor for daily usage. Existing EMG sensing technique is not applicable in our goal of capturing the movement of corrugator muscle group. The reason is that the corrugator supercillii is smaller than other action units related to pain as stated in Section 2. Thus, its activities are overlapped by other AUs' activities.

We introduce Sweep Impedance Profiling (SIP), a technique that measures the impedance of surface muscles using multiple AC 'active' signals; and infers directly the movement of the muscle groups. This sensing method requires to put only two electrodes over the position of that muscle. In our case of the corrugator supercillii, these two electrode positions are easy to located by identifying (i) the middle of the eyebrow and (ii) the junction between eyebrow and eyesocket (next to the middle of two eyebrows called glabella). After capturing the responses to these AC signals, we are able to analyze the relation between muscle impedance and muscle length. Combining multiples measurements from that AC frequency range provides a rich feature profile of the selected muscle group.

**Impedance of human body part.** The impedance  $Z$  of an object is given by:  $Z = R + jX$  where  $R$  is the resistance and  $X$  is the combination of capacitance  $X_C$  and inductance  $L$  of the given object. In human-body-related applications, inductance plays a minimal role in standard impedance measurement [91], so the imaginary impedance component can be simplified to  $X = X_C = 1/2\pi fC$ , where  $f$  is the excitation frequency. As a result, total impedance magnitude  $|Z|$  and impedance phase  $\phi$  of a human body part will be calculated as:

$$|Z| = \sqrt{R^2 + X_C^2}, \phi = \tan^{-1}(X_C/R) \quad (1)$$

**Relation of muscle impedance to muscle movement.** We model the muscle as a solid cylinder with length of  $L$  and radius of  $r$ . The muscle resistance and self capacitance will be calculated as follows:

$$R = \rho(L/A), C = \left(8 + 4.1(L/r)^{0.76}\right) \epsilon_m r \quad (2)$$

where  $\rho$  is the muscle resistivity coefficient,  $A$  is a cross-sectional area, and  $\epsilon_m$  is overall muscle permittivity.

The intuition given by Eq. 1 and 2 is that the dimensions of the muscle will change due to muscle activity (e.g., the autonomic innervation of corrugator muscle in our scenario). In addition,  $R$  and  $C$  behave differently based on the change of muscle dimensions  $L$ ,  $r$ , and  $A$ . This leads to the non-linear changes of total impedance  $Z$  due to muscle activity. Due to the dependence of  $Z$  on excitation frequency  $f$ , sweeping through a wide range of excitation frequencies will provide corresponding values of  $Z(f)$  and yield a 'profile' of the selected muscle group.

Fig. 4 shows the anatomy of facial muscle related to the corrugator supercillii area under four layers of skin, subcutaneous fat, frontalis muscle, and corrugator muscle. Since we care about corrugator muscle, the corresponding basic sweeping circuit consists of four impedances as shown in Fig. 4. In this model,  $Z_{E1S}$  and  $Z_{E2S}$  are dependant on the contact between electrode and skin and are calibrated using lead-off-detection (mentioned later in Sec. 6). Thus, sweeping excitation frequency  $f$  over a short period achieves the corresponding impedance profile of corrugator muscle group under different pain states.

**DFT-based impedance measurement.** Among various impedance measurement technique, we choose the Discrete Fourier Transform (DFT) technique [28]. This method provides the best calculation accuracy of an unknown impedance while requires smallest memory space in hardware realization [56]. It correlates the captured AC signal with sinusoidal basis functions, which are both sine and cosine waveforms. This correlation results in a complex numeric value, in which the imaginary and real parts represent the correlation of the signal with the sine and cosine waveforms, respectively. From this value, its magnitude is used to compute the magnitude spectrum, and its phase value is used to obtain the phase spectrum. Specifically, given the excitation signal:  $v_S(t) = V_0 \cos(2\pi ft + \theta)$

The real  $RE$  and imaginary  $IM$  parts of each sample  $i \in [0..N-1]$  after the DFT correlation process is:

$$\begin{cases} RE_i = \frac{2}{N} \sum_{n=0}^{N-1} \left[ v_i(nT) \cos\left(\frac{2\pi}{N}n\right) \right] \\ IM_i = \frac{2}{N} \sum_{n=0}^{N-1} \left[ v_i(nT) \sin\left(\frac{2\pi}{N}n\right) \right] \end{cases} \quad (3)$$

where  $T$  is sampling interval and  $N$  is the number of sample respectively.

Magnitude and phase of the unknown impedance  $Z$  will be calculated as following with reference resistor  $R$ :

$$|Z| = \frac{\sqrt{RE_Z^2 + IM_Z^2}}{\sqrt{RE_R^2 + IM_R^2}}, \phi = \tan^{-1}\left(\frac{RE_Z IM_R - RE_R IM_Z}{RE_Z RE_R + IM_Z IM_R}\right) \quad (4)$$

DFT-based measurement provides accurate impedance measurement but has large numbers of sampling and calculation requirement to store the above resulting  $RE$  and  $IM$  components [56] (i.e. high processing power). We mitigate this drawback with our choice of hardware components (Section 6). Fig. 4 shows the feasibility of capturing the movement of corrugator supercillii using SIP under the sweeping range 10 kHz to 100 kHz (covers the known frequency for surface impedance analyzer [73]). The safety design and integration of SIP with other conventional sensors (EEG, PPG, and GSR) will be discussed in the next section.

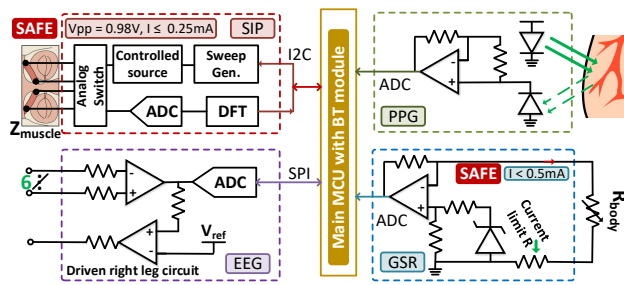


Figure 5: Painometry hardware schematic.

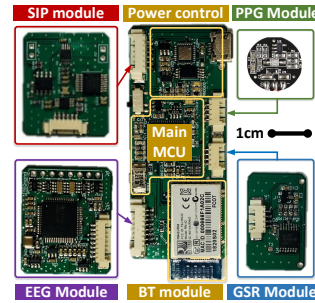


Figure 6: Fabricated PCBs.



Figure 7: Sensor placements in various Painometry form-factors.

## 5 PAINOMETRY HARDWARE DESIGN

### 5.1 Design considerations

**Safety consideration.** Since our customized SIP and GSR sensors are considered ‘active’ (i.e., they excite electrical signals to parts of the human body), special precautions need to be implemented to ensure user’s safety. According to ICNIRP guidelines [36, 74] and IEEE C95.1 standard [4], 1mA is considered a safety threshold for DC and AC signals having the frequency below 1MHz. As a result, our SIP sensor has been configured so that it has the output AC of  $0.98 V_{pp}$  and maximum output current of  $0.25 mA$ . Moreover, the AC signal from SIP must not interfere with the brain signal frequencies recorded by EEG sensor, i.e., the frequency must be larger than  $1 kHz$  [32]. The GSR sensor is designed to restrict the DC signal to  $1.2 V$  applied directly to human skin. Furthermore, the GSR sub-circuit output current is limited at  $0.5 mA$  by a current-limit resistor.

**Hardware noise reduction.** There are three main hardware noise sources in our system: (1) electromagnetic noises from the surrounding environment coupling into the signal wires and human body, (2) parasitic noise from electrical components in the sensing sub-circuit itself, and (3) cross-talk noise induced by high-speed digital components into the analog domain. The EEG acquisition module provides a driven right leg circuit [116] which helps to eliminate common-mode noise coupled into the human body. To further increase the signal-to-noise ratio, we put the amplifiers of sensing circuits close to the point of measurement, and the wires are kept as short as possible. Additionally, all of the electrical components used to construct Painometry hardware are high precision with low tolerance level. We designed SIP sensors to operate at high frequency ( $10 kHz - 100 kHz$ ) in order to avoid the superposition on meaningful frequency bands of EEG (i.e. below  $100 Hz$ ). We also add the low-pass filter RC on EEG and GSR sub-circuit to eliminate the effect of high-frequency AC signals from SIP generator.

Cross-talk noise between digital and analog sources is alleviated by ground separation in hardware design including (i) separation of the analog ground domain and digital ground domain and (ii) separation between each sub-circuit as depicted in Fig. 6. Furthermore, the SIP measurements of the two corrugator groups are processed sequentially to avoid interference from 2 AC sweep sources. Thus, the SIP sub-circuit utilizes an analog switch to consecutively interchange the SIP measurement between the two muscle groups.

### 5.2 Implementation

Fig. 5 shows the overview of Painometry hardware schematic with the corresponding SIP, EEG, PPG, and GSR modules. and Fig. 6 shows the corresponding fabricated PCBs. Fig. 8 shows the example of the change in sensing data captured by Painometry multimodal sensing hardware under the influence of pain-inducing stimulation experiment (the details of experimental protocol are in Sec. 7)

**SIP sensor module.** We built a SIP sensor from the high-resolution impedance analyzer AD5933 [1] and the low noise op-amp AD8606 [2]. To measure SIP from 2 corrugator muscles sequentially, we use the analog switch TS5A23159 [105] and four electrode montages over eyebrows. The SIP sensor sweeps 10 excitation signals over the range of  $10kHz$  to  $100kHz$  at  $0.98 V_{pp}$  and maximum output current of  $0.25 mA$ .

**EEG sensor module.** We built an EEG sensor module with the core as TI-ADS1299, the ultra-low noise amplifiers with internal noise at  $1\mu V$  (peak-to-peak). This module can check the electrode-skin contact impedance using lead-off detection to ensure high-quality signals before the recording. This feature is also used to measure  $Z_{E1S}$  and  $Z_{E2S}$  in the SIP circuit model to calibrate the SIP measurement. EEG hardware uses ten electrodes including 6 EEG channels (T3-T4, Fp1-Fp2, and F7-F8), one reference, and one bias. The location of reference and bias electrodes depend on the form-factor of Painometry, i.e. T5-T6 in a hat or a headband; and at the temple tips of the eye-glass form-factor.

**GSR sensor module.** We built a GSR sensor based on a non-inverting amplifying circuit with the single micro-power precision amplifier LMP2231 [61] and a precision micro-power shunt voltage reference LM4041 [60]. The GSR sensor uses two electrode montages on top of the forehead. The gain resistor was tuned so that the swing range of GSR output expands as much as possible in the ADC reading range of the main MCU. The GSR sub-circuit output current is limited at  $0.5 mA$  by a current-limit resistor.

**PPG sensor module.** We use the reference design of a pulse sensor [83]. In this design, there is a super-bright green LED used with the dominant wavelength at  $525nm$  accompanied by a highly sensitive light sensor to pick up reflected light from the artery. The green LED and light sensor are placed in the middle of the forehead as discussed in Sec. 2.

**Putting together Painometry.** We use the TI MSP432P401R [70] as the main MCU which connects to SIP sensor via I2C, to EEG

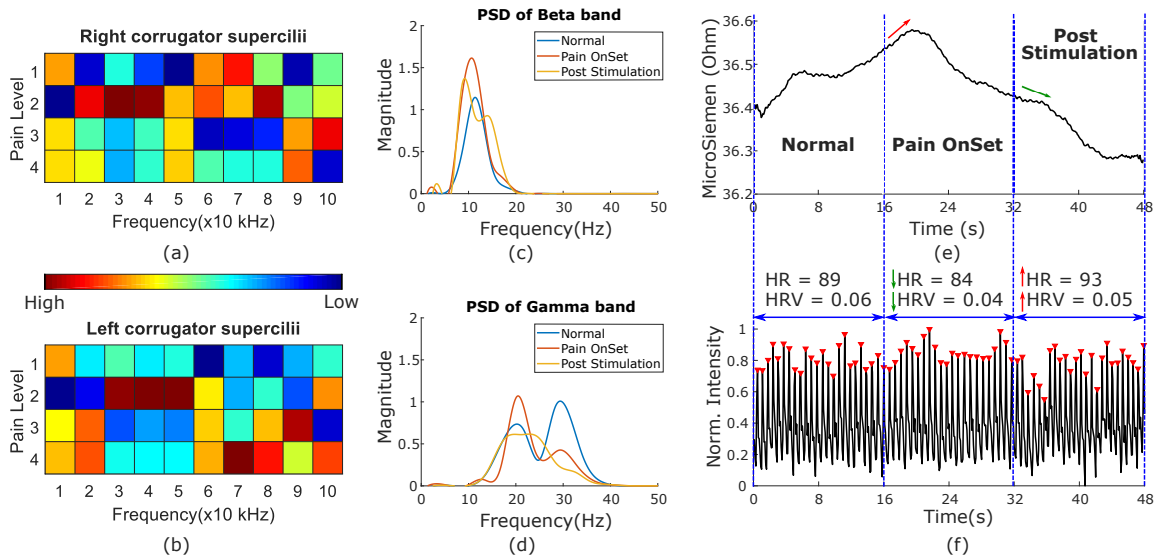


**Figure 8: Painometry sensor measurements: (a-b) Normalized average SIP measurement with different pain levels; (c-d) Power Spectrum Density envelope of gamma and beta bands in EEG from T4 montage; (e) GSR and (f) PPG measurement with peak detection of HR/HRV trend in experimental pain stimulation.**

sensor via SPI, and to GSR, PPG sensor via analog I/O. This low-power MCU has enough high performance to satisfy SIP computing requirement. Sensor measurements are then broadcasted out via a Bluetooth module [87]. Finally, we mount all electrodes and both hardware PCBs onto a Velcro flexible patch, which can be easily mounted on various form factors such as a hat, a headband, or an eye-glass. Fig. 7 shows the sensor placements on those form-factors. While both SIP sensors (4 electrodes in total) can be mounted on eye-glass, in other 2 form-factors, those sensors are adjusted on-the-fly with 2 floating electrodes (not shown in the figure). Fig 9 shows the whole hardware modules and sensor connection assembled on a headband, which we use for our experiment and evaluation.

## 6 OBJECTIVE PAIN QUANTIFICATION

### 6.1 Signal Pre-Processing

In Painometry, we analyze signals collected from four sensing sources: SIP, EEG, GSR, and PPG. Each signal is pre-processed differently due to the differences in their respective signal properties such as frequencies of interest, sampling rate, and noise effects before they are passed through the feature analysis pipeline (Sec. 7.2).

**Signal cleaning process.** Even with our effort in minimizing hardware noise as presented in the previous section, the raw sensing data is still prone to noise including (1) DC drifting, (2) 50/60Hz power line interference, and (3) user movement artifacts. Hence, we continuously process raw data using an overlapped sliding window. We initially apply a spline interpolation method so that all measurements have the same length. We then remove the DC linear trend of each window (except GSR measurement) by subtracting the 6th-order polynomial fit from the original signals. The reason GSR is left out is because useful information such as the tonic component (skin conductance level) can be extracted from the DC

trend. Finally, we apply a notch filter to further suppress 50/60Hz power line interference and lowpass filters of 1Hz and 100Hz to the PPG and EEG signal, respectively, to remove unexpected movement artifacts.

**EEG decomposition.** Pain features spread across different regions of the frequency domain (i.e., Alpha, Beta, Gamma, Delta, Theta) [50, 53, 75]. As a result, a single frequency band does not fully capture the brain’s response to pain. Therefore, decomposing signals into multiple frequency bands facilitates more distinctive features to be extracted. Classical approaches have used bandpass filters to extract different frequency bands. However, applying a bandpass filter causes low-frequency background drift, spoils the endpoints of the signal, and may lead to the loss of crucial details about acute pain. Fourier transform [8] is another common attempt that breaks down the signal into a sum of sinusoidal base functions in order to determine the signal’s spectral components. However, since these sinusoidal base functions are, by design, infinite signals in the time domain, this method results in the loss of temporal information when each frequency band is reconstructed in the time domain. Wavelet decomposition [31], on the other hand, is better suited for non-stationary signals which may vary instantaneously in time [23], as do the biosignals recorded here. Thus, we leverage this approach and apply a 6th-order Daubechies 9 wavelet decomposition to extract the five frequency bands of interest from the cleaned EEG signal.

**Peak detection and HR/HRV calculation.** Each heartbeat creates a peak that can be seen clearly in each PPG window. Thus, we apply a peak detection algorithm onto a sliding sub-window. After that, the heart rate variability (HRV) is calculated by taking the standard deviation of all the heartbeat interval inside a chunk data. The sub-window slides overlap until they find a local peak above the magnitude threshold. Then the sub-window skips the

sliding over this heartbeat interval and look for the local peak of the next heartbeat interval.

## 6.2 Pain Features Extraction

After obtaining and pre-processing the EEG, GSR, PPG, and SIP signals, the collected time series data from each source is segmented to fixed-size epochs, and selected features are extracted from each epoch to be used for classification of the pain level in that epoch. In the following sections, we present the feature selection and classification steps in our pain level quantification pipeline. Informed by the literature, the features selected for extraction from each signal are from a variety of categories as follows:

**Temporal features.** This category includes statistical features for time series data analysis, namely, mean, variance, skewness, and kurtosis. In pain classification, both GSR and SIP signals are often analyzed in time domain due to their considerable variation in amplitude and lack of distinctive frequency patterns [27, 101]. Hence, those four temporal features are extracted from single GSR channel and ten channels of SIP. Furthermore, since heart rate changes when one experiences the pain [104], we choose heart rate variability as one independent temporal feature. Overall, there are 45 temporal features extracted (i.e., 4 GSR, 40 SIP, and 1 HRV).

**Spectral features.** The spectral features are extracted to analyze the characteristics of EEG signal because brain waves are generally available in discrete frequency ranges at different stages [59, 110]. By transforming the time series EEG signal into the frequency domain in different frequency bands (i.e., Theta, Alpha, Sigma, Beta, and Gamma) and computing its power spectrum density, various spectral features can be extracted. All the spectral features are extracted from the EEG signals at T3, T4, Fp1, and Fp2 channels, which include the ratio of powers, absolute powers, theta/gamma, theta/alpha, and sigma/gamma. Accordingly, 13 features are extracted from each of the four channels of EEG, which provides 52 spectral features in total.

**Non-linear features.** Bioelectrical signals show various complex behaviors with nonlinear properties. In particular, the chaotic parameters of EEG can be used for pain level classification. The discriminant ability of nonlinear analyses of EEG dynamics is demonstrated through the measures of complexity such as correlation dimension, Lyapunov exponent, entropy, fractal dimension, etc. [100], with the last two features proven to be most informative. In this study, we extract these two non-linear features for each of the EEG channels (a total of 8 features).

Tab. 1 summarizes the features we extract from each type of signal under each category of features in this study.

## 6.3 Pain Feature Selection

Even though each extracted feature can capture certain characteristics of the input signals, the performance of a classification algorithm can be degraded when all possible features are used together, mainly due to feature redundancy. In particular, some of the features may be irrelevant or redundant, further reducing the classification accuracy.

In order to select a set of relevant features among the 105 extracted features, we need to compute the discriminating ability of each feature when they are used in combination. However, it is

Type	Signal	Feature
Temporal	GSR, SIP	-mean, variance -skewness, kurtosis
Temporal	PPG	-heart rate variability
Spectral	EEG	-absolute spectral powers -relative spectral powers -relative spectral ratio
Non-linear	EEG	-fractal dimension, entropy

**Table 1: List of pain features**

computationally infeasible to test all of possible combinations. To identify the most effective combination of features, we adopt three feature selection methods, namely, Recursive Feature Elimination (RFE), L1-based feature selection, and tree-based feature selection. RFE [14] is a greedy optimization algorithm that seeks to improve generalization performance of the classification model by removing the least important features whose deletion will have the least effect on training error. L1-based feature selection [55] is used for linear models including Logistic Regression and Support Vector Machines (SVM). Since we apply these linear models during the classification process, we use L1 norm to remove features with coefficients of zero. Finally, with tree-based feature selection [30] takes a different approach by computing importance of features which in turn is used to remove irrelevant features.

## 6.4 Pain Level Classification

Various classification methods including the Support Vector Machine (SVM), Logistic Regression, Decision Tree and Random Forest have been proposed in literature for pain or stress level detection, each shown to be effective in specific settings [27, 110]. To be inclusive, we deploy all these models in this study and perform an empirical comparative analysis to identify the best performing model for our pain level identification system (see Sec. 7 for our experimental results).

**Sample fusion based GMM:** The acute pain feeling remains the same over a short period; hence, we perform a fusion approach to combine the data in one period to improve the performance. We explore the use of the GMM feature aggregation technique to encode 16 data signals into one sample. For each epoch of data, we train the GMM model using the Expectation-Maximization (EM) algorithm. The means of GMM is concatenated to form the sample data for this signal.

## 7 PERFORMANCE EVALUATION

Here, we discuss in detail the set of experiments conducted to evaluate the overall performance of Painometry. Also, we evaluate our proposed SIP sensor performance to demonstrate its ability to capture the autonomous muscle movements. In particular, we evaluate the following aspects: (1) reliability and safety of the experiment protocol, (2) performance of pain quantification pipeline, and (3) user experience survey. We deployed the classification model on a Google Pixel 2 [29]. The average runtime is about 0.17 ms per classification along with 14% CPU usage and 75MB memory usage.

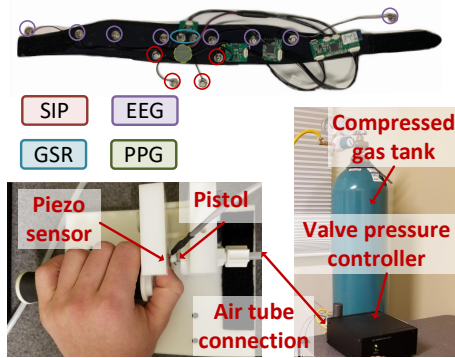


Figure 9: Painometry headband form-factor and pain-inducing experiment setup

## 7.1 Experimental Methodology

Our experimental design goals are (1) inducing clearly distinguishable pain levels in order to get true labels for the ground truth of 4 different pain states (i.e. no-pain and 3 pain levels), (2) avoiding the effects of short-term pain tolerance, and (3) ensuring the safety of the experimental conditions. Since we understand the goals, complexity, and unpleasantness of this research study, our experimental pain-inducing device and protocol has been thoroughly designed and approved by the Institutional Review Board (IRB) of University of Colorado, Boulder. Participant demographics are shown in Table 2. All subjects in our study were pre-screened to be pain-free at the time of experiment, i.e. no chronic pain.

Existing pain-related research has used various methods to induce experimental pain such as pressure pain [11, 15, 42], thermal pain [21, 41] and cold pain [114]. Each method has its own unpleasantness and side effects after the experiment (e.g. bruise after pressure pain, skin burnt after thermal pain or allergy after cold pain). We chose pressure pain induced on subjects' thumbs as our experimental pain method because we can guarantee the development of acute pain (similar to postoperative acute pain) with a clear distinction between different pain levels. Also, this method has a low probability of producing side effects (3 bruises reported from 20 subjects in our pilot study and 23 subjects in our research study).

Participant Demographics	
Age (years)	21 - 52 years old
Participant groups	20 in pilot study, 23 subjects
Pain states	4 (pain-free and 3 levels of pain)
Data collection	12 pain-inducing runs, random order
Bruise after experiment	9.1% (3 subjects)

Table 2: Data collection details.

**Pressure pain device (PPD).** The PPD is designed to be safe and accurate in delivering experimental pain. This device includes the mechanical pain delivery component (with a piston-like front-end), the pressure controller hardware and a compressed air tank as shown in Fig. 9. The device is designed with a handle to keep the hand comfortable and still while receiving pressure. A hardware

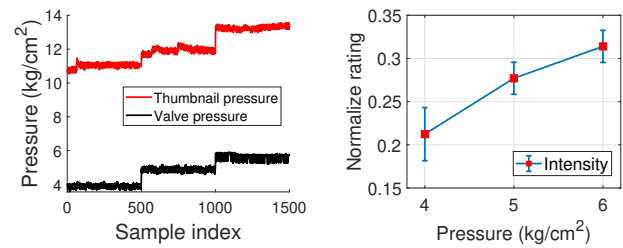


Figure 10: PPD pressure validation

Figure 11: Average rating across subjects

pressure regulator limits pressure to below  $14 \text{ kg/cm}^2$  to prevent excessive pressure. Pressure intensity and duration are controlled by our LabView implementation. PPD tracks both valve pressure and piston-to-thumb nail pressure level in real-time. To ensure the safety of the device and experimental protocol, the mechanical pain delivery component is held together by 2 asymmetrical screws which gives subjects the ability to remove their thumbs at their discretion.

**Pain stimulation protocol.** The protocol is designed to deliver clear distinct pain levels to the subject and to avoid the effects of short-term pain tolerance. We use PPD to create 3 different pain levels of mild, moderate, and strong. Each subject will experience 12 stimulation runs (i.e. 4 runs for each pain level) in a pseudo-random sequence. Each run is divided into 3 intervals: T1 (before the stimulus) is first and lasts 16 seconds, T2 (pain stimulus onset) is next and lasts 16 seconds, and T3 (after the pain stimulus ceased) lasts 30 seconds at least. During the experiment, the Painometry headband records the subjects' biosignals through all the runs. The subjects rate their pain subjectively using the VAS scale right after T2. In addition, T3 is adjusted on-the-fly in order to ensure the subjects' thumb returns to normal feeling before each stimulation run. Fig. 10 and Fig. 11 prove the correctness and reliability of PPD in delivering pain perceptions and shows the corresponding valve pressure levels, thumbnail pressure levels, and average normalized pain rating for each pressure level across 23 subjects. The pressure applied on the subjects' thumb nail scales proportionally to 3 valve pressure levels. The average pain rating shows the correlation of pressure levels to the subjects' rating on stimulation runs.

## 7.2 System Performance

We evaluated the performance of our proposed SIP sensing method and pain quantification pipeline using the accuracy, precision, and recall as performance measures. First, we evaluated the impact of using different feature selection approaches, using each Painometry sensor in isolation. Then we performed Leave-one-out cross validation (LOOCV) to evaluate classification accuracy on 2 data sets: (i) 3 pain levels (no-pain, mild, and strong pain) and (ii) 4 pain levels (no-pain, mild, moderate, and strong pain). During each iteration of LOOCV, 22 of 23 subjects' data are used to train our model and the remaining one is used to validate the prediction pain level. This process is repeated for all 23 subjects to estimate the accuracy on the unseen data. Towards this end, we use accuracy, precision, and recall as performance measures.

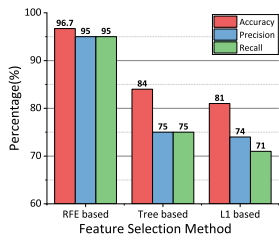


Figure 12: Impact of feature selection methods

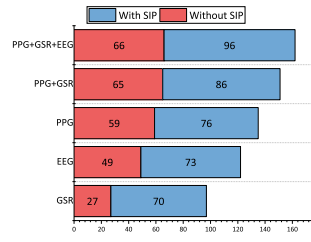


Figure 13: Impact of sensor combinations

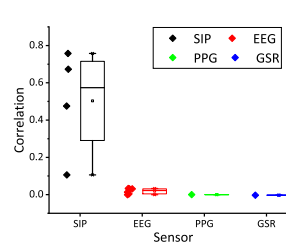


Figure 14: Correlation coefficients

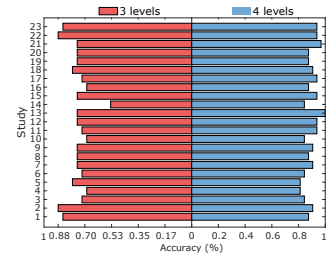


Figure 15: Accuracy across subjects

We first evaluated the performance of various feature selection methods by performing the data-split validation on our data set. Fig. 12 displays accuracy when the features are selected from the RFE, Tree-based, and L1-based approaches. The result shows that RFE with Decision Tree provides the best accuracy of 96.7% among the combination of feature selection methods and classifiers.

To study the expressive power of the features extracted in our pipeline, we calculated the correlation between each of the extracted features and the pain levels using the *cor* package in R [52]. As illustrated in Fig. 14, the features extracted from the SIP signal have the highest correlation with the pain levels with a mean of 0.6. Features from the EEG, PPG, and GSR signals ranked in the second, third, and fourth, respectively.

	Sensing Method	Level	Accuracy
[110]	EEG	2	95.3%
[12]	fMRI	2	84%
[95]	EEG	2	78.5%
Painometry	SIP, EEG, GSR, PPG	3	89.5%
[71]	EEG	3	83%
[65]	GSR	3	77.4%
[47]	Video, EMG, GSR	4	83.1%
Painometry	SIP, EEG, GSR, PPG	4	76.7%
[16]	GSR, ECG	4	75%
[112]	fMRI	5	84.2%
[71]	EEG	5	62%

Table 3: Leave-one-out cross validation performance comparison with some notable existing works

In our next evaluation, represented by Fig. 13, we studied how using different combinations of biosignal sensors would impact the classification accuracy. In order to test the feasibility and impact of SIP sensor, we also quickly perform the data-split validation on our data set. As illustrated, using only GSR and PPG signals can classify the pain levels at an accuracy of 27% and 59% without the SIP, respectively. On the other hand, considering only EEG or three signals of PPG, GSR, and EEG without SIP signal can achieve an accuracy of 49% and 66%, respectively. Consequently, it proves the feasibility that SIP sensor has a high impact on improving the accuracy.

The top features as ranked by RFE demonstrate most distinguishing power for classification include a variety of SIP features (ranked

highest), followed by heart rate variability, a number of EEG at T3 and T4 channels, and GSR mean. We used this feature set for the rest of our LOOCV evaluation.

Fig. 16, 17, 18 show the average performance of 3 and 4 pain level quantification respectively using different classification method including Logistic Regression (LR), Decision Tree (DT), Support Vector Machines (SVM), Random Forest Classifier (RFC), and XGBC. As illustrated, the maximum accuracy of 89.5% and 76.7% is achieved using DT and RFC for 3 and 4 pain levels respectively among different classification methods. On the other hand, the LR method provides the least accuracy on both data set of 75.14% and 67.39%. Fig. 15 shows the accuracy from each subjects.

Tab. 3 shows the comparison of our system to other quantification methods of experimental pain based on state-of-the-art laboratory sensing systems using fMRI and biosignal sensors. Given our wearable device, we are able to achieve pain quantification accuracy for 3 and 4 levels on par with those previous works. This shows that the Painometry provides reasonable and reliable results.

**Painometry hardware power profiling.** We used the Monsoon power measurement tool [69] to validate the power consumption of current Painometry prototype. At operating voltage of 3.3 V, our fabricated hardware has an average power consumption of 292.1 mW in the active state (measuring sensor and streaming data via Bluetooth), and (2) 56.8 mW in idle state (only MCU running in sleep mode). Using a 500-mAh battery can maintain the Painometry hardware for 5.6 hours in the active state continuously. The sensing sub-circuits and Bluetooth communication module have the highest power consumption of 129.4 mW and 93.7 mW respectively. In order to fit the needs of all-day usage, we can further increase the operation duration of Painometry by optimizing hardware components (i.e. MCU, external ADCs, and BLE with lower power consumption) and larger sized battery.

### 7.3 User study

While developing and evaluating Painometry, we also conducted a survey to identify gaps in our system and the expectations of the users (both users with the experience of wearing Painometry during the experiment and prospective users). This information provides us the insight to improve Painometry in the future.

We distributed our survey to 35 people, including our 23 subjects and 12 subjects who had no prior experience with Painometry. Fig. 19 shows five questions we asked and the statistics on our participants’ answers. Specifically, analyzing the result of Question

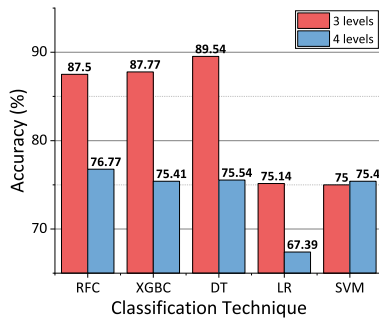


Figure 16: Average accuracy.

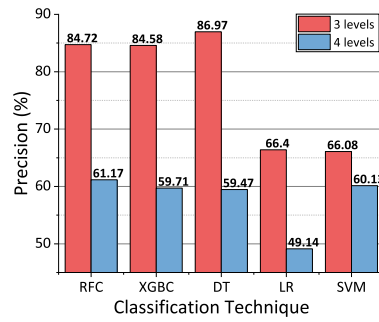


Figure 17: Average precision.

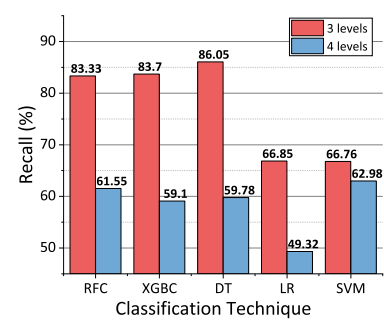


Figure 18: Average recall.

“How hard is it for you to quantify your pain objectively?” shows that it is not easy for everyone to objectively rate their pain. From Questions “When was the last time you had to / you struggled to rate your pain?”, we see that 11 out of 35 participants experienced pain within a week; and nearly 80% of them struggled to rate it. As a result, this statistics demonstrates a need for the objective pain quantifier.

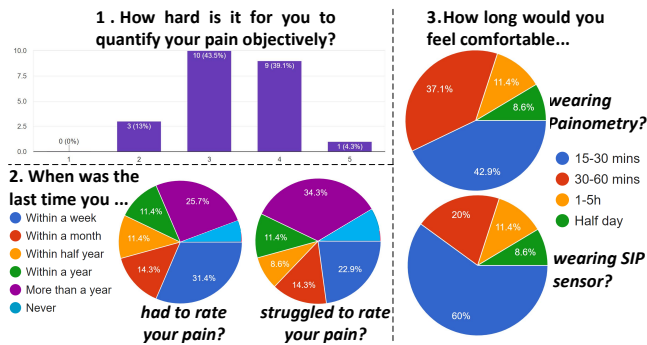


Figure 19: User study results

Finally, we studied how long people are willing to wear a headband-like device with the placement of sensors on their forehead and around their head during the use. The answers to the question, “How long would you feel comfortable wearing Painometry and SIP sensor?”, suggest that people can tolerate to wear such a device and sensors for 15-30 minutes at most. This information helps know the need of improving the comfort of our current design as well as building a timing constraint in a pain intervention system.

## 8 RELATED WORK

**Pain quantification systems.** There have been various systems relying on either single or multiple sensing modalities to quantify pain [33, 35, 43, 50, 53, 66, 67, 71, 75, 90, 96, 102, 113]. In [53], Kumar et al. proposed an EEG-based system that can quantify the patient’s physiological response to pain under general anaesthesia. In this system, the authors developed a real-time pain index based on an easy-to-access biosignal. Using the same EEG input, Kagita et al. [50] proposed a binary classification of whether the user has pain or not with an accuracy of 100%. However, this model was not

cross-validated or tested on a new dataset. Consequently, it suffers from overfilling to be considered as a reliable tool for pain classification. Besides the use of frequency band power, [71] extracted more features including fractal dimension, Shannon entropy, approximate entropy, and spectral entropy and achieved around 62-83% accuracy in detection of 3 or 5 pain levels. Another commercial product in this single sensing modality group is the PainQx system [75], which has developed a source localization algorithm for improved analysis of EEG data of pain patients. Different than the aforementioned systems, Seok et al. [96] focused on proposing a set of optimized algorithms for a continuous postoperative pain assessment tool based on the analysis of a pulse contour of PPG signal.

To further enrich the pain quantification resolution, many systems have been developed to measure other signal types such as skin conductance [102], facial features [35, 90], heart rate variability (HRV) [43], and trunk strength [66]. Specifically, [33, 113] advanced the automated pain recognition system with various biopotential data including EEG, EMG, ECG, and skin conductance level. Salah et al. [92], otherwise, proposed a system that fuses geometric facial expressions and physiological signals to quantify pain. It captures both similar physiological signals and analyzes the movements of many of the facial muscles emphasized in the FACS manual [22]. The system also relies on a unique algorithm incorporating a SVM linear model and video signal databases. In the same use case of where patients are unable to communicate as [53], PMD-200™ [67, 68] pain monitoring device developed by Medasense company, on the other hand, is a tool that uses a derivation from the nonlinear composite of heart rate (HR), HR variability, amplitude of the photoplethysmogram, skin conductance, fluctuations in skin conductance, and their time derivatives to define a novel multidimensional index of nociception, the nociception level (NOL) index.

Additionally, several patents also applied the concept of quantifying pain by measuring various vital signals and movements [3, 44, 82]. These patents describe endeavors to integrate an extensive range of noninvasive methods for monitoring patients’ daily physiological and environmental stressors in objective, quantifiable schemes via portable devices. The integration of multiple signals has become a trending solution to boost the performance of high-resolution pain quantification systems. However, to collect multiple signals, form factors are cumbersome, uncomfortable, and require many accessories, which make systems unusable in daily life. In

contrast to existing systems, our system is light-weight and requires a minimal number of sensors.

**Muscle profiling techniques.** Applying AC currents to determine the impedance of body tissues actively has already existed. It has been widely used in various healthcare applications. Existing technology is relatively simple, effective, fast, and noninvasive. Its most popular application is to estimate body composition [26, 63, 97], which typically uses 50 kHz AC at less than 1mA. Multi-frequency measurements, or a frequency spectrum, are also being used to evaluate differences in body composition caused by different clinical and nutritional conditions [49, 76, 109]. Another application of this technology is to determine muscle diseases. In [7], the authors used this technology to predict skeletal muscle mass. Meanwhile, it is also an alternative for myography, which is a study of the velocity and intensity of muscular contraction [7, 58, 93, 98].

Though SIP shares the same fundamental principle of impedance-based profiling with the aforementioned techniques, its advantages lie in the abilities to (1) measure impedance of the singular muscle group under skin, (2) provide more detailed information about the muscle over a range of sweeping excitation frequencies, and (3) specify with greater precision the area of muscle of interest.

## 9 DISCUSSION

**Chronic pain vs. Acute pain.** We have shown the effectiveness of using Painometry in classifying different experimental acute pain levels, allowing for more objective monitoring of indicators of acute postoperative pain during a critical period in the rehabilitation process. Since there is a strong correlation between the severity of acute postoperative pain and development of chronic pain [80], the algorithm and feature selection of physiological expressions (i.e., SIP, EEG, PPG, GSR) in this paper will be useful as we extend Painometry to chronic pain quantification. Since the existing experimental stimulation device does not support mobility, we plan to design and seek permission for new protocol before evaluating Painometry with in-the-wild scenario in the near future.

**Limitation.** The target of Painometry system in this work is classifying different experimental acute pain levels in the controlled in-lab experiment setup. Thus, the system at the current state is prone to false positives from the frown expression Painometry. While the SIP method has the advantage of capturing the movement of the targeted group muscle only (i.e. corrugator supercilli) and Painometry can address motion and environmental noises, there are several artifacts that pose as challenges to its usability in the real world. In particular, frown expression and sweating can introduce noises into the SIP and GSR measurement respectively. It is part of our future work to optimize the sensors and system in order to enhance the practicality of the system.

**Application to a range of form factors.** Furthermore, we have demonstrated in this work the versatility of the Painometry electrode arrangement in its application to a range of unique form factors. Presumably, the convenience of offering the system in a range of wearable form factors ensures repeated and continued use during the postoperative recovery period.

**Towards a closed-loop pain intervention system.** The Painometry system has the potential to be applicable in rehabilitation

settings, contributing to interventional therapies that bypass medication schedules used to relieve long-term pain. A recent study similarly interested in developing an automatic, objective measurement of signals indicating chronic pain has been successful in recognizing and classifying video recordings of pain-related movements and facial expressions in a group of chronic pain patients [5].

Once we are able to classify different pain levels based on biosignals, the next logical step would be to analyze the transition between pain states taking into account the biopsychosocial model of pain. Such a model can provide insights on not only the physiological markers of pain transition but also the psychological triggers of pain. This has the potential to help predict pain episodes before they happen and further develop a closed-loop, just-in-time, and drug-free pain coaching system.

## 10 CONCLUSION

In this work, we propose Painometry, a wearable system that provides automated and pain quantification in daily life. Notably, the Painometry prototype captures the changes in multiple biosignals from the subject during pain. Based on our research and understanding of the anatomy and physiology of pain, we have designed Painometry to model the relations between pain and the recorded biosignals. From the relations observed, we have established different pain quantification levels. The Painometry prototype has been evaluated on 23 subjects (8832 data points from 276 minutes) through an IRB-approved pain-inducing protocol, and show 89.5% and 76.7% accuracy of pain quantification under 3 and 4 pain states respectively. Finally, Painometry is our first step in targeting chronic pain quantification, detecting psychological pain triggers, and developing a fully closed-loop ‘just-in-time’ pain intervention system.

**Acknowledgements.** We thank Dr. Sung-Ju Lee for serving as the shepherd for the paper and the reviewers for their insightful comments. We also thank Mr. Art Atkison for his consultancy in the writing of this paper. Our research was partially funded by NSF CNS/CSR #1846541, NSF SCH #1602428.

## REFERENCES

- [1] AD5933 [n.d.]. AD5933 12-Bit Impedance Converter. <https://www.analog.com/en/products/ad5933.html>.
- [2] AD8606 [n.d.]. Precision, Low Noise, RRIO, CMOS Op Amp (Dual) AD8606. <https://www.analog.com/en/products/ad8606.html#product-overview>.
- [3] Elizabeth Mary Annoni, Jianwen Gu, Pramodsingh Hirasingsh Thakur, Bryan Allen Clark, and Kyle Harish Srivastava. 2018. Patient-specific calibration of pain quantification. US Patent App. 15/867,772.
- [4] ANSI ANSI. 1992. IEEE C95. 1-1992: IEEE Standard for Safety Levels with Respect to Human Exposure to Radio Frequency Electromagnetic Fields, 3 kHz to 300 GHz, The Institute of Electrical and Electronics Engineers. Inc., New York, NY 10017 (1992).
- [5] Min S. H. Aung, Sebastian Kaltwang, Bernardino Romera-Paredes, Brais Martinez, Aneeha Singh, Matteo Cella, Michel Valstar, Hongying Meng, Andrew Kemp, Moshen Shafizadeh, Aaron C. Elkins, Natalie Kanakam, Amschel de Rothschild, Nick Tyler, Paul J. Watson, Amanda C. de C Williams, Maja Pantic, and Nadia Bianchi-Berthouze. 2016. The Automatic Detection of Chronic Pain-Related Expression: Requirements, Challenges and the Multimodal EmoPain Dataset. *IEEE transactions on affective computing* 7, 4 (2016), 435–451. <https://doi.org/10.1109/TAFFC.2015.2462830> 30906508[pmid].
- [6] Hyun Jae Baek, Haet Bit Lee, Jung Soo Kim, Jong Min Choi, Ko Keun Kim, and Kwang Suk Park. 2009. Noninvasive biological signal monitoring in a car to evaluate a driver’s stress and health state. *Telemedicine and e-Health* 15, 2 (2009), 182–189.

- [7] A Bony-Westphal, B Jensen, W Braun, M Pourhassan, D Gallagher, and MJ Müller. 2017. Quantification of whole-body and segmental skeletal muscle mass using phase-sensitive 8-electrode medical bioelectrical impedance devices. *European journal of clinical nutrition* 71, 9 (2017), 1061.
- [8] Ronald Newbold Bracewell and Ronald N Bracewell. 1986. *The Fourier transform and its applications*. Vol. 31999. McGraw-Hill New York.
- [9] Gabriel A Brat, Denis Agniel, Andrew Beam, Brian Yorkgits, Mark Bicket, Mark Homer, Kathe P Fox, Daniel B Knecht, Cheryl N McMahlil-Walraven, Nathan Palmer, and Isaac Kohane. 2018. Postsurgical prescriptions for opioid naive patients and association with overdose and misuse: retrospective cohort study. *BMJ* 360 (2018). <https://doi.org/10.1136/bmj.j5790> arXiv:<https://www.bmj.com/content/360/bmj.j5790.full.pdf>
- [10] Harald Breivik, PC Borchgrevink, SM Allen, LA Rosseland, L Romundstad, EK Breivik Hals, G Kvarstein, and A Stubhaug. 2008. Assessment of pain. *BJA: British Journal of Anaesthesia* 101, 1 (2008), 17–24.
- [11] Jannick Brennum, Michel Kjeldsen, Kai Jensen, and Troels Staehelin Jensen. 1989. Measurements of human pressure-pain thresholds on fingers and toes. *Pain* 38, 2 (1989), 211–217.
- [12] Justin E Brown, Neil Chatterjee, Jarred Younger, and Sean Mackey. 2011. Towards a physiology-based measure of pain: patterns of human brain activity distinguish painful from non-painful thermal stimulation. *PLoS one* 6, 9 (2011), e24124.
- [13] Robert G Carlson, Ramzi W Nahhas, Silvia S Martins, and Raminta Daniulaityte. 2016. Predictors of transition to heroin use among initially non-opioid dependent illicit pharmaceutical opioid users: A natural history study. *Drug and alcohol dependence* 160 (2016), 127–134.
- [14] X. Chen and J. C. Jeong. 2007. Enhanced recursive feature elimination. In *Sixth International Conference on Machine Learning and Applications (ICMLA 2007)*. 429–435. <https://doi.org/10.1109/ICMLA.2007.35>
- [15] Linda S Chesterton, Panos Barlas, Nadine E Foster, G David Baxter, and Christine C Wright. 2003. Gender differences in pressure pain threshold in healthy humans. *Pain* 101, 3 (2003), 259–266.
- [16] Yaqi Chu, Xingang Zhao, Jianda Han, and Yang Su. 2017. Physiological signal-based method for measurement of pain intensity. *Frontiers in neuroscience* 11 (2017), 279.
- [17] Theodore J Cicero, Matthew S Ellis, Hilary L Surratt, and Steven P Kurtz. 2014. The changing face of heroin use in the United States: a retrospective analysis of the past 50 years. *JAMA psychiatry* 71, 7 (2014), 821–826.
- [18] Kenneth D. Craig, Susan A. Hyde, and Christopher J. Patrick. 1991. Genuine, suppressed and faked facial behavior during exacerbation of chronic low back pain. *Pain* 46, 2 (1991), 161–171. [https://doi.org/10.1016/0304-3959\(91\)90071-5](https://doi.org/10.1016/0304-3959(91)90071-5)
- [19] Philip De Chazal, Niall Fox, EMER O'HARE, Conor Heneghan, Alberto Zaffaroni, Patricia Boyle, Stephanie Smith, CAROLINE O'CONNELL, and Walter T McNicholas. 2011. Sleep/wake measurement using a non-contact biomotion sensor. *Journal of sleep research* 20, 2 (2011), 356–366.
- [20] Philip De Chazal, Emer O'Hare, Niall Fox, and Conor Heneghan. 2008. Assessment of sleep/wake patterns using a non-contact biomotion sensor. In *2008 30th Annual International Conference of the IEEE Engineering in Medicine and Biology Society*. IEEE, 514–517.
- [21] Robert R Edwards and Roger B Fillingim. 1999. Ethnic differences in thermal pain responses. *Psychosomatic medicine* 61, 3 (1999), 346–354.
- [22] Paul Ekman and Wallace V. Friesen. 1978. *Facial Action Coding System: Manual*.
- [23] Burhan Ergen. 2012. *Signal and Image Denoising Using Wavelet Transform*. <https://doi.org/10.5772/36434>
- [24] W Paul Farquhar-Smith. 2008. Anatomy, physiology and pharmacology of pain. *Anaesthesia & intensive care medicine* 9, 1 (2008), 3–7.
- [25] Centers for Disease Control, Prevention, et al. 2016. Wide-ranging online data for epidemiologic research (WONDER). *Atlanta, GA: National Center for Health Statistics* (2016).
- [26] Maria Franco-Villoria, Charlotte M Wright, John H McColl, Andrea Sherriff, Mark S Pearce, Gateshead Millennium Study core team, et al. 2016. Assessment of adult body composition using bioelectrical impedance: comparison of researcher calculated to machine outputted values. *BMJ open* 6, 1 (2016), e008922.
- [27] A. Ghaderi, J. Frounchi, and A. Farnam. 2015. Machine learning-based signal processing using physiological signals for stress detection. In *2015 22nd Iranian Conference on Biomedical Engineering (ICBME)*. 93–98. <https://doi.org/10.1109/ICBME.2015.7404123>
- [28] Victor Giurgiutiu and Buli Xu. 2004. Development of a field-portable small-size impedance analyzer for structural health monitoring using the electromechanical impedance technique. In *Smart Structures and Materials 2004: Sensors and Smart Structures Technologies for Civil, Mechanical, and Aerospace Systems*, Vol. 5391. International Society for Optics and Photonics, 774–786.
- [29] googlepixel [n.d.]. Google Pixel 2 XL. [https://store.google.com/sg/product/pixel\\_2\\_xl](https://store.google.com/sg/product/pixel_2_xl)
- [30] Krzysztof Grabczewski and Norbert Jankowski. 2005. Feature selection with decision tree criterion. 6 pp. <https://doi.org/10.1109/ICHS.2005.43>
- [31] Amara Graps. 1995. An introduction to wavelets. *IEEE computational science and engineering* 2, 2 (1995), 50–61.
- [32] Nir Grossman, David Bono, Nina Dedic, Suhasa B Kodandaramaiah, Andrii Rudenko, Ho-Jun Suk, Antonino M Cassara, Esra Neufeld, Niels Kuster, Li-Huei Tsai, et al. 2017. Noninvasive deep brain stimulation via temporally interfering electric fields. *Cell* 169, 6 (2017), 1029–1041.
- [33] Sascha Gruss, Roi Treister, Philipp Werner, Harald C Traue, Stephen Croucher, Adriano Andrade, and Steffen Walter. 2015. Pain intensity recognition rates via biopotential feature patterns with support vector machines. *PLoS one* 10, 10 (2015), e0140330.
- [34] Ying Gu, Evy Cleeren, Jonathan Dan, Kasper Claes, Wim Van Paesschen, Sabine Van Huffel, and Borbála Hunyadi. 2018. Comparison between scalp EEG and behind-the-ear EEG for development of a wearable seizure detection system for patients with focal epilepsy. *Sensors* 18, 1 (2018), 29.
- [35] MJ Guesgen, NJ Beausoleil, M Leach, EO Minot, M Stewart, and KJ Stafford. 2016. Coding and quantification of a facial expression for pain in lambs. *Behavioural processes* 132 (2016), 49–56.
- [36] ICNIRP Guideline. 1998. Guidelines for limiting exposure to time-varying electric, magnetic, and electromagnetic fields (up to 300 GHz). *Health phys* 74, 4 (1998), 494–522.
- [37] Jennifer M. Hah, Brian T. Bateman, John Ratliff, Catherine Curtin, and Eric Sun. 2017. Chronic Opioid Use After Surgery: Implications for Perioperative Management in the Face of the Opioid Epidemic. *Anesthesia & Analgesia* 125, 5 (2017), 1733–1740.
- [38] Gillian A Hawker, Samra Mian, Tetyana Kendzerska, and Melissa French. 2011. Measures of adult pain: Visual analog scale for pain (vas pain), numeric rating scale for pain (nrs pain), mcgill pain questionnaire (mpq), short-form mcgill pain questionnaire (sf-mpq), chronic pain grade scale (cpgs), short form-36 bodily pain scale (sf-36 bps), and measure of intermittent and constant osteoarthritis pain (icoap). *Arthritis care & research* 63, S11 (2011), S240–S252.
- [39] Matthew S Herbert, Burel R Goodin, Samuel T Pero IV, Jessica K Schmidt, Adriana Sotolongo, Hailey W Bulls, Toni L Glover, Christopher D King, Kimberly T Sibille, Yenisel Cruz-Almeida, et al. 2013. Pain hypervigilance is associated with greater clinical pain severity and enhanced experimental pain sensitivity among adults with symptomatic knee osteoarthritis. *Annals of Behavioral Medicine* 48, 1 (2013), 50–60.
- [40] Richard W Homan, John Herman, and Phillip Purdy. 1987. Cerebral location of international 10–20 system electrode placement. *Electroencephalography and clinical neurophysiology* 66, 4 (1987), 376–382.
- [41] Clara Huihui Zhang, Abbas Sohrabpour, Yunfeng Lu, and Bin He. 2016. Spectral and spatial changes of brain rhythmic activity in response to the sustained thermal pain stimulation. *Human brain mapping* 37, 8 (2016), 2976–2991.
- [42] Kai Jensen, Henrik Ørbaek Andersen, Jes Olesen, and Ulf Lindblom. 1986. Pressure-pain threshold in human temporal region. Evaluation of a new pressure algometer. *Pain* 25, 3 (1986), 313–323.
- [43] Gunnar Jess, Esther M Pogatzki-Zahn, Peter K Zahn, and Christine H Meyer-Frieem. 2016. Monitoring heart rate variability to assess experimentally induced pain using the analgesia nociception index: A randomised volunteer study. *European Journal of Anaesthesiology (EJA)* 33, 2 (2016), 118–125.
- [44] Erwin Roy John, Leslie S Pritchep, and Emile Hiesiger. 2016. System and method for pain detection and computation of a pain quantification index. US Patent 9,402,558.
- [45] Christopher M Jones. 2013. Heroin use and heroin use risk behaviors among nonmedical users of prescription opioid pain relievers—United States, 2002–2004 and 2008–2010. *Drug and alcohol dependence* 132, 1–2 (2013), 95–100.
- [46] Markus Kächele, Mohammadreza Amirian, Patrick Thiam, Philipp Werner, Steffen Walter, Günther Palm, and Friedhelm Schwenker. 2017. Adaptive confidence learning for the personalization of pain intensity estimation systems. *Evolving Systems* 8, 1 (2017), 71–83.
- [47] Markus Kächele, Patrick Thiam, Mohammadreza Amirian, Friedhelm Schwenker, and Günther Palm. 2016. Methods for person-centered continuous pain intensity assessment from bio-physiological channels. *IEEE Journal of Selected Topics in Signal Processing* 10, 5 (2016), 854–864.
- [48] Markus Kächele, Philipp Werner, Ayoub Al-Hamadi, Günther Palm, Steffen Walter, and Friedhelm Schwenker. 2015. Bio-visual fusion for person-independent recognition of pain intensity. In *International Workshop on Multiple Classifier Systems*. Springer, 220–230.
- [49] MW Kafri, JF Potter, and PK Myint. 2014. Multi-frequency bioelectrical impedance analysis for assessing fat mass and fat-free mass in stroke or transient ischaemic attack patients. *European journal of clinical nutrition* 68, 6 (2014), 677.
- [50] Junichiro Kagita and Yasue Mitsukura. 2018. Quantification of pain degree by frequency features of single-channelled EEG. In *2018 IEEE 15th International Workshop on Advanced Motion Control (AMC)*. IEEE, 359–363.
- [51] Kyriaki Kalimeri and Charalampos Saitis. 2016. Exploring multimodal biosignal features for stress detection during indoor mobility. In *Proceedings of the 18th ACM International Conference on Multimodal Interaction*. ACM, 53–60.
- [52] Maurice G Kendall. 1938. A new measure of rank correlation. *Biometrika* 30, 1/2 (1938), 81–93.
- [53] Sanjeev Kumar, Amod Kumar, Anjan Tripathi, and Sneha Anand. 2015. Electroencephalogram based quantitative estimation of pain for balanced anaesthesia.

- Measurement* 59 (2015), 296 – 301. <https://doi.org/10.1016/j.measurement.2014.09.021>
- [54] Karim S. Ladha. 2019. Opioid Prescribing After Surgery in the United States, Canada, and Sweden. *JAMA Network Open* 2, 9 (09 2019), e1910734–e1910734. <https://doi.org/10.1001/jamanetworkopen.2019.10734> arXiv:[https://jamanetwork.com/journals/jamanetworkopen/articlepdf/2749239/ladha\\_2019\\_o](https://jamanetwork.com/journals/jamanetworkopen/articlepdf/2749239/ladha_2019_o)
- [55] Su-In Lee, Honglak Lee, Pieter Abbeel, and Andrew Y. Ng. 2006. Efficient L1 Regularized Logistic Regression. In *AAAI*.
- [56] Grzegorz Lentka. 2014. Using a particular sampling method for impedance measurement. *Metrology and Measurement Systems* 21, 3 (2014), 497–508.
- [57] Linda LeResche and Samuel F. Dworkin. 1988. Facial expressions of pain and emotions in chronic TMD patients. *Pain* 35, 1 (1988), 71 – 78. [https://doi.org/10.1016/0304-3959\(88\)90278-3](https://doi.org/10.1016/0304-3959(88)90278-3)
- [58] Xiaoyan Li, Le Li, Henry Shin, Sheng Li, and Ping Zhou. 2017. Electrical impedance myography for evaluating parietic muscle changes after stroke. *IEEE Transactions on Neural Systems and Rehabilitation Engineering* 25, 11 (2017), 2113–2121.
- [59] Manyoel Lim, June Sic Kim, Dajung J Kim, and Chun Kee Chung. 2016. Increased low-and high-frequency oscillatory activity in the prefrontal cortex of fibromyalgia patients. *Frontiers in human neuroscience* 10 (2016), 111.
- [60] LM4041 [n.d.]. LM4041 Precision Micropower Shunt Voltage Reference. <http://www.ti.com/product/LM4041-N>.
- [61] LMP2231 [n.d.]. LMP2231 Precision Operational Amplifier with CMOS Inputs. <http://www.ti.com/product/LMP2231>.
- [62] Daniel Lopez-Martinez and Rosalind Picard. 2018. Continuous Pain Intensity Estimation from Autonomic Signals with Recurrent Neural Networks. In *2018 40th Annual International Conference of the IEEE Engineering in Medicine and Biology Society (EMBC)*. IEEE, 5624–5627.
- [63] Henry C Lukaski, Phyllis E Johnson, William W Bolonchuk, and Glenn I Lykken. 1985. Assessment of fat-free mass using bioelectrical impedance measurements of the human body. *The American journal of clinical nutrition* 41, 4 (1985), 810–817.
- [64] Mark A Lumley, Jay L Cohen, George S Borszcz, Annmarie Cano, Alison M Radcliffe, Laura S Porter, Howard Schubiner, and Francis J Keefe. 2011. Pain and emotion: a biopsychosocial review of recent research. *Journal of clinical psychology* 67, 9 (2011), 942–968.
- [65] Gordon Matthewson, Choong-Wan Woo, Marianne C Reddan, and Tor D Wager. 2019. Cognitive self-regulation influences pain-related physiology. *bioRxiv* (2019), 361519.
- [66] TG Mayer, SUSAN S Smith, JANICE Keeley, and VERT Mooney. 1985. Quantification of lumbar function. Part 2: Sagittal plane trunk strength in chronic low-back pain patients. *Spine* 10, 8 (1985), 765–772.
- [67] Medasense Biometrics Ltd. [n.d.]. PMD-200 - Pain Monitoring Device. <https://tinyurl.com/sxf9cac>.
- [68] Fleur S Meijer, Chris H Martini, Suzanne Broens, Martijn Boon, Marieke Nesters, Leon Aarts, Erik Olofsen, Monique van Velzen, and Albert Dahan. 2019. Nociception-guided versus Standard Care during Remifentanyl-Propofol Anesthesia: A Randomized Controlled Trial. *Anesthesiology: The Journal of the American Society of Anesthesiologists* 130, 5 (2019), 745–755.
- [69] Moonson [n.d.]. Moonson Power Management Tool. <https://goo.gl/f9j3Dz>.
- [70] MSP432P401R [n.d.]. TI MSP432P401R MCU. <http://www.ti.com/product/MSP432P401R>.
- [71] Tahereh Nezam, Reza Boostani, Vahid Abootalebi, and Karim Rastegar. 2018. A Novel Classification Strategy to Distinguish Five Levels of Pain using the EEG Signal Features. *IEEE Transactions on Affective Computing* (2018).
- [72] Anh Nguyen, Raghda Alqurashi, Zohreh Raghebi, Farnoush Banaei-Kashani, Ann C Halbower, and Tam Vu. 2016. A lightweight and inexpensive in-ear sensing system for automatic whole-night sleep stage monitoring. In *Proceedings of the 14th ACM Conference on Embedded Network Sensor Systems CD-ROM*. ACM, 230–244.
- [73] Nile M Oldham. 1996. Overview of bioelectrical impedance analyzers. *The American journal of clinical nutrition* 64, 3 (1996), 405S–412S.
- [74] International Commission on Non-Ionizing Radiation Protection et al. 2003. Guidance on determining compliance of exposure to pulsed and complex non-sinusoidal waveforms below 100 kHz with ICNIRP guidelines. *Health physics* 84, 3 (2003), 383–387.
- [75] painqx [n.d.]. The PainQx System - Objective and Quantitative Pain Measurement. <https://www.painqx.com/>.
- [76] K Panorchan, A Nongnuch, S El-Kateb, C Goodlad, and A Davenport. 2015. Changes in muscle and fat mass with haemodialysis detected by multi-frequency bioelectrical impedance analysis. *European journal of clinical nutrition* 69, 10 (2015), 1109.
- [77] Leonard J Paulozzi. 2012. Prescription drug overdoses: a review. *Journal of safety research* 43, 4 (2012), 283–289.
- [78] HC Philips. 2015. Imagery and likelihood cognitive bias in pain. *Behavioural and cognitive psychotherapy* 43, 3 (2015), 270–284.
- [79] Tamar Pincus and Stephen Morley. 2001. Cognitive-processing bias in chronic pain: a review and integration. *Psychological bulletin* 127, 5 (2001), 599.
- [80] WA Pluijms, MAH Steegers, AFTM Verhagen, GJ Scheffer, and OHG Wilder-Smith. 2006. Chronic post-thoracotomy pain: a retrospective study. *Acta anaesthesiologica scandinavica* 50, 7 (2006), 804–808.
- [81] Kenneth M. Prkachin and Susan R. Mercer. 1989. Pain expression in patients with shoulder pathology: validity, properties and relationship to sickness impact. *Pain* 39 (1989), 257 – 265. [https://doi.org/10.1016/0304-3959\(89\)90038-9](https://doi.org/10.1016/0304-3959(89)90038-9)
- [82] Christopher L Pulliam and Joseph P Giuffrida. 2017. Pain quantification and management system and device, and method of using. US Patent 9,782,122.
- [83] pulsesensor [n.d.]. Open-Source Pulse Sensor Hardware. <https://pulsesensor.com/>.
- [84] Marianne C Reddan and Tor D Wager. 2018. Modeling pain using fMRI: from regions to biomarkers. *Neuroscience bulletin* 34, 1 (2018), 208–215.
- [85] P. Reicherts, A. B. Gerdes, P. Pauli, and M. J. Wieser. 2013. On the mutual effects of pain and emotion: facial pain expressions enhance pain perception and vice versa are perceived as more arousing when feeling pain. *Pain* 154, 6 (Jun 2013), 793–800.
- [86] Philipp Reicherts, Matthias J. Wieser, Antje B. M. Gerdes, Katja U. Likowski, Peter Weyers, Andreas Mühlberger, and Paul Pauli. 2012. Electrocutaneous evidence for preferential processing of dynamic pain expressions compared to other emotional expressions. *PAIN* 153, 9 (2012). [https://journals.lww.com/pain/Fulltext/2012/09000/Electrocutaneous\\_evidence\\_for\\_preferential.26.aspx](https://journals.lww.com/pain/Fulltext/2012/09000/Electrocutaneous_evidence_for_preferential.26.aspx)
- [87] RN42 [n.d.]. Microchip RN42 Bluetooth Module. <https://www.microchip.com/wwwproducts/en/RN42>.
- [88] Rosa Rojo, Juan Carlos Prados-Frutos, and Antonio López-Valverde. 2015. Pain assessment using the Facial Action Coding System. A systematic review. *Medicina Clínica (English Edition)* 145, 8 (2015), 350 – 355. <https://doi.org/10.1016/j.medcle.2014.08.002>
- [89] Robert Rosenthal and Ralph L Rosnow. 1984. Applying Hamlet’s question to the ethical conduct of research: A conceptual addendum. *American Psychologist* 39, 5 (1984), 561.
- [90] Sourav Dey Roy, Mrinal Kanti Bhowmik, Priya Saha, and Anjan Kumar Ghosh. 2016. An Approach for Automatic Pain Detection through Facial Expression. *Procedia Computer Science* 84 (2016), 99 – 106. Proceeding of the Seventh International Conference on Intelligent Human Computer Interaction (IHCI 2015).
- [91] Seward B Rutkove. 2009. Electrical impedance myography: background, current state, and future directions. *Muscle & Nerve: Official Journal of the American Association of Electrodiagnostic Medicine* 40, 6 (2009), 936–946.
- [92] Amir Salah, Mahmoud I Khalil, and Hazem Abbas. 2018. Multimodal Pain Level Recognition using Majority Voting Technique. In *2018 13th International Conference on Computer Engineering and Systems (ICCES)*. IEEE, 307–312.
- [93] Benjamin Sanchez and Seward B Rutkove. 2017. Electrical impedance myography and its applications in neuromuscular disorders. *Neurotherapeutics* 14, 1 (2017), 107–118.
- [94] Stephan A Schug, Patricia Lavand’homme, Antonia Barke, Beatrice Korwisi, Winfried Rief, Rolf-Detlef Treede, et al. 2019. The IASP classification of chronic pain for ICD-11: chronic postsurgical or posttraumatic pain. *Pain* 160, 1 (2019), 45–52.
- [95] Enrico Schulz, Andrew Zherdin, Laura Tiemann, Claudia Plant, and Markus Ploner. 2011. Decoding an individual’s sensitivity to pain from the multivariate analysis of EEG data. *Cerebral cortex* 22, 5 (2011), 1118–1123.
- [96] Hyeon Seok, Byung-Moon Choi, Gyu-Jeong Noh, and Hangsik Shin. 2019. Post-operative Pain Assessment Model Based on Pulse Contour Characteristics Analysis. *IEEE Journal of Biomedical and Health Informatics* PP (11 2019), 1–1. <https://doi.org/10.1109/JBHI.2018.2890482>
- [97] Giuseppe Sergi, Marina De Rui, Brendon Stubbs, Nicola Veronese, and Enzo Manzato. 2017. Measurement of lean body mass using bioelectrical impedance analysis: a consideration of the pros and cons. *Aging clinical and experimental research* 29, 4 (2017), 591–597.
- [98] Carl A Shiffman, Ronald Aaron, and Seward B Rutkove. 2015. Electrical impedance myography. US Patent 9,014,797.
- [99] Lee S Simon. 2012. Relieving pain in America: A blueprint for transforming prevention, care, education, and research. *Journal of pain & palliative care pharmacotherapy* 26, 2 (2012), 197–198.
- [100] Carolina Sitges, Xavier Bornas, Jordi Labrés, Miquel Noguera, and Pedro Montoya. 2010. Linear and nonlinear analyses of EEG dynamics during non-painful somatosensory processing in chronic pain patients. *International Journal of Psychophysiology* 77, 2 (2010), 176–183.
- [101] Jair Stern, Daniel Jeanmonod, and Johannes Sarnthein. 2006. Persistent EEG overactivation in the cortical pain matrix of neurogenic pain patients. *Neuroimage* 31, 2 (2006), 721–731.
- [102] Hanne Storm. 2008. Changes in skin conductance as a tool to monitor nociceptive stimulation and pain. *Current Opinion in Anesthesiology* 21, 6 (2008), 796–804.
- [103] Abdulhamit Subasi and M Kemal Kiyimik. 2010. Muscle fatigue detection in EMG using time–frequency methods, ICA and neural networks. *Journal of medical systems* 34, 4 (2010), 777–785.

- [104] Astrid Juhl Terkelsen, Henning Molgaard, John Hansen, Ole Kaeseler Andersen, and Troels Staehelin Jensen. 2005. Acute pain increases heart rate: Differential mechanisms during rest and mental stress. *Autonomic Neuroscience* 121 (2005), 101–109.
- [105] TS5A23159 [n.d.]. TS5A23159 2:1 Multiplexer / Demultiplexer. <http://www.ti.com/product/TS5A23159>.
- [106] Yiheng Tu, Yeung Sam Hung, Zhiguo Zhang, and Li Hu. 2014. Prediction of pain perception using multivariate pattern analysis of laser-evoked EEG oscillations. In *Control Automation Robotics & Vision (ICARCV), 2014 13th International Conference on*. IEEE, 13–16.
- [107] Marieke van Dooren, Joris H Janssen, et al. 2012. Emotional sweating across the body: Comparing 16 different skin conductance measurement locations. *Physiology & behavior* 106, 2 (2012), 298–304.
- [108] Carolina Varon, Katrien Jansen, Lieven Lagae, and Sabine Van Huffel. 2015. Can ECG monitoring identify seizures? *Journal of electrocardiology* 48, 6 (2015), 1069–1074.
- [109] Julien Verney, Chloé Schwartz, Saliha Amiche, Bruno Pereira, and David Thivel. 2015. Comparisons of a multi-frequency bioelectrical impedance analysis to the dual-energy X-ray absorptiometry scan in healthy young adults depending on their physical activity level. *Journal of human kinetics* 47, 1 (2015), 73–80.
- [110] Vishal Vijayakumar, Michelle Case, Sina Shirinpour, and Bin He. 2017. Quantifying and Characterizing Tonic Thermal Pain Across Subjects From EEG Data Using Random Forest Models. *IEEE Transactions on Biomedical Engineering* 64, 12 (2017), 2988–2996.
- [111] Kevin E Vowles, Mindy L McEntee, Peter Siyahhan Julnes, Tessa Frohe, John P Ney, and David N van der Goes. 2015. Rates of opioid misuse, abuse, and addiction in chronic pain: a systematic review and data synthesis. *Pain* 156, 4 (2015), 569–576.
- [112] Tor D Wager, Lauren Y Atlas, Martin A Lindquist, Mathieu Roy, Choong-Wan Woo, and Ethan Kross. 2013. An fMRI-based neurologic signature of physical pain. *New England Journal of Medicine* 368, 15 (2013), 1388–1397.
- [113] Steffen Walter, Sascha Gruss, Kerstin Limbrecht-Ecklundt, Harald C Traue, Philipp Werner, Ayoub Al-Hamadi, Nicolai Diniz, Gustavo Moreira da Silva, and Adriano O Andrade. 2014. Automatic pain quantification using autonomic parameters. *Psychology & Neuroscience* 7, 3 (2014), 363.
- [114] Gunnar Wasner, JoÈrn Schattschneider, Andreas Binder, and Ralf Baron. 2004. Topical menthol—a human model for cold pain by activation and sensitization of C nociceptors. *Brain* 127, 5 (2004), 1159–1171.
- [115] Suzanne Wendelken, Susan McGrath, George Blike, and Metin Akay. 2004. The feasibility of using a forehead reflectance pulse oximeter for automated remote triage. In *IEEE 30th Annual Northeast Bioengineering Conference, 2004. Proceedings of the IEEE*, 180–181.
- [116] Bruce B Winter and John G Webster. 1983. Driven-right-leg circuit design. *IEEE Transactions on Biomedical Engineering* 1 (1983), 62–66.